

Transition from a molecular to a metallic adsorbate system: Core-hole creation and decay dynamics for CO coordinated to Pd

A. Sandell* and J. Libuda[†]

Lehrstuhl für Physikalische Chemie I, Ruhr-Universität-Bochum, D-44780 Bochum, Germany

P. A. Brühwiler and S. Andersson

Department of Physics, Uppsala University, Box 530, 751 21 Uppsala, Sweden

M. Bäumer[†]

Lehrstuhl für Physikalische Chemie I, Ruhr-Universität-Bochum, D-44780 Bochum, Germany

A. J. Maxwell and N. Mårtensson

Department of Physics, Uppsala University, Box 530, 751 21 Uppsala, Sweden

H.-J. Freund[†]

Lehrstuhl für Physikalische Chemie I, Ruhr-Universität-Bochum, D-44780 Bochum, Germany

(Received 8 July 1996; revised manuscript received 15 October 1996)

Two alternative methods to experimentally monitor the development of a CO-adsorption system that gradually changes from molecular to metallic are presented: firstly by adsorption of CO on Pd islands of increasing size deposited under UHV conditions, and secondly by growth of a Pd carbonyl-like species, formed by Pd deposition in CO atmosphere. The change in screening dynamics as a function of the number of metal atoms was investigated, using x-ray photoelectron spectroscopy, x-ray absorption spectroscopy, and core-hole-decay techniques. For CO adsorbed on UHV-deposited islands, the electronic properties of the whole CO-Pd complex is strongly dependent on island size and CO coverage: large amounts of CO result in a reduced screening ability, and small effects characteristic of molecular systems can be detected even for islands containing about 100 Pd atoms. If about half of the CO overlayer is desorbed, the CO-Pd complex exhibits a relaxation upon core ionization that is nearly as efficient as for metallic systems, even for the smallest islands (of the order of 10 Pd atoms). The growth of the carbonyl-like compound proceeds via formation of Pd-Pd bonds and has a relatively well-defined local structure. It is demonstrated that the properties of this compound approach those of an extended system for increasing coverages, and it may therefore also serve as an important link between a carbonyl and CO adsorbed on a metallic surface. A brief discussion is also given in which the results are discussed in terms of electronic properties of the thin alumina film versus bulk alumina and the applicability of the former to the construction of model catalysts. [S0163-1829(97)04111-8]

I. INTRODUCTION

The adsorption of molecules on metal surfaces constitutes one of the most fundamental issues in surface science. Upon adsorption, the electronic levels of the molecule become strongly modified, and a detailed knowledge of the electronic structure is vital for an understanding of adsorption energies, adsorption geometries, chemical properties, etc. In this context, questions regarding electron correlation, charge transfer, and screening response upon ionization have attracted a lot of attention.¹ Electron excitation and decay dynamics are furthermore important within the field of photoinduced processes such as desorption and dissociation.¹

For extended, metallic systems, a detailed understanding of all these properties is not easily achieved due to the large number of electronic levels involved, although results employing cluster calculations and band-structure models have been rather successful. An important step towards a more complete understanding of the adsorption bond was taken by introducing complexes consisting of molecules bonded to only a few metal (Me) atoms as intermediates. In the case of

CO, which is the prototype adsorbate, experimental data on carbonyls were found to exhibit many features similar to the CO/Me case: The valence photoemission spectra show a clear tendency for an energy degeneracy of the 5σ and 1π levels, which is a typical feature for chemisorbed CO.² Moreover, the so-called shakeup satellites observed in the core-level photoemission spectra for carbonyls have been successfully identified using theoretical calculations.^{3,4} These results in turn provide clues as to the origin of the satellites in the spectra for CO adsorbed on metal surfaces.^{2,4-11} Another important example is that the Auger spectra for carbonyls nicely demonstrate that charge-transfer screening into the CO $2\pi^*$ orbital occurs upon core ionization, leading to spectral shapes very similar to those observed for CO on metals.^{12,13}

However, there are still significant differences between the carbonyl data and the results for CO on metals, e.g., the shakeup satellites are much broader for CO/Me (Refs. 4-11) and the so-called spectator shift between the Auger electron (AE) spectrum and the autoionization (AI) spectrum [the latter is also denoted deexcitation electron (DE) or resonant

Auger spectrum], which is observed for carbonyls, is absent for CO chemisorbed on metal surfaces.^{14–16} Both these properties are likely connected to the size of the system, but there are so far no investigations that, for example, clearly show how many metal atoms are needed in order to quench the spectator shift. Another problem is the limited number of carbonyls; i.e., several CO/Me systems cannot be modeled simply because there exist no stable carbonyl compounds containing the metal of interest. It is therefore obvious that there is a need to find alternative ways to fill the gap between a molecular system and a large, extended adsorption system.

In this paper, we present two different approaches to this issue: firstly by studying CO adsorbed on metal (Pd) islands of different size deposited onto a thin alumina film under UHV conditions and secondly by studying the successive growth of a carbonyl-like compound [$\text{Pd}_x(\text{CO})_y$] formed by Pd deposition in CO atmosphere. Both growth modes have been extensively characterized previously, using photoemission of core and valence levels, thermal desorption spectroscopy (TDS), and SPA-LEED (spot profile analysis–low-energy electron diffraction).^{17–21} Employing (high-resolution) core-level spectroscopies, we have now investigated these systems in order to elucidate how the screening dynamics of a CO-Pd complex change with the number of metal atoms and amount of CO. X-ray photoelectron spectroscopy (XPS) and x-ray absorption spectroscopy (XAS) were used to determine the screening response for a fast process (i.e., “the sudden limit”) whereas AES and AIS were used to investigate the screening dynamics on the time scale of the core-hole lifetime (10^{-15} s).

For the UHV-deposited islands, we find that the screening dynamics is strongly dependent on both island size and CO coverage: Adsorption of large amounts of CO leads to CO-Pd complexes with a screening ability lower than for the clean Pd islands, and small effects typical for carbonyl molecules can be detected even for islands containing approximately 100 Pd atoms. In the case of low CO coverage, however, a screening nearly as efficient as for metallic systems is observed even for the smallest islands (of the order of 10 Pd atoms). The growth of the $\text{Pd}_x(\text{CO})_y$ compound evidently proceeds via formation of Pd-Pd bonds. It has a relatively well-defined local structure and new, complementary data concerning the CO adsorption geometries are presented. The results furthermore clearly show that this compound becomes more similar to an extended system when the deposited amount increases.

II. EXPERIMENT

The experiments were carried out at beamline 22 at the Swedish synchrotron radiation facility MAX-lab in Lund. The setup contains a modified Zeiss SX-700 monochromator in conjunction with a large hemispherical electron energy analyzer for photoemission and a multichannel plate with a retarding grid for x-ray absorption measurements by detection of secondary electrons.²² The C 1s XP spectra were recorded at a photon energy of 380 eV with a total resolution set to 0.4 eV. The Pd 3d XP spectra were recorded at a photon energy of 420 eV and a resolution of 0.3 eV. All the XPS binding energies (BE) are referred to the Fermi level of the NiAl(110) substrate. The XA spectra were measured in

partial yield mode with a photon energy resolution of 0.2 eV at both the C 1s and the O 1s edges. Fortunately, the CO-related O 1s XAS peaks were easy to separate from the oxide features, thereby allowing for a subtraction of the latter. The absolute photon energies (PE) were determined using photoemission spectra excited by first- and second-order radiation. The C 1s AI spectra were recorded with a photon energy resolution of 0.2 eV and an electron energy resolution of 0.6 eV.

The preparation of the clean NiAl(110) surface and the oxidation procedure to form a well-ordered Al_2O_3 film have been described elsewhere.²³ This film has furthermore been extensively investigated employing several different techniques.^{23,24} Pd was evaporated using a Knudsen cell and the evaporation rate was monitored using a quartz microbalance. We will henceforth use the nominal film thicknesses as obtained by the quartz microbalance to denote the different situations. The $\text{Pd}_x(\text{CO})_y$ compound was formed by evaporation of Pd with a CO background pressure of 5×10^{-6} Torr onto the sample, which was cooled down to 90 K.

III. RESULTS AND DISCUSSION

A. CO adsorbed on supported Pd particles

The growth of Pd on the thin alumina film under UHV conditions is described in detail elsewhere.^{17,19} Briefly, deposition of Pd at 90 K results in the formation of poorly ordered three-dimensional (3D) islands. This is the case for the 0.2- and 2.0-Å situations in the present study. Deposition of 12-Å Pd at 300 K, however, results in large crystallites dominated by (111) facets. For the following discussion, it is most important to have at least a rough idea about how large the islands are, and a simple estimation for the 0.2-Å case yields that the average island has a diameter of about 5 Å and therefore consists of about 10 Pd atoms. The corresponding numbers for the 2.0- and 12-Å situations are (20 Å)/(100 atoms) and (60 Å)/(2000 atoms), respectively.²⁵

Two different situations with adsorbed CO were investigated: A high-coverage phase obtained by dosing 30 L [1 L (langmuir) = 10^{-6} Torr s] CO at a sample temperature of 90 K and a low-coverage phase obtained by heating the previous phase to 300 K, which leads to desorption of 50–60% of the CO. The previous studies, using XPS, XAS, and TDS, demonstrated that the CO-Pd interaction strength increases with increasing cluster size and decreasing CO coverage.^{20,21} It should furthermore be noted that the heating procedure does not drastically change the size or structure of the islands.²¹

1. Core excitation and core ionization

It is well known that the chemical bonding of CO onto a transition-metal surface involves a hybridization between the CO $2\pi^*$ orbital and the Me d levels. The interaction is manifested in the XA spectrum as a broadening of the core-to- $2\pi^*$ peak (i.e., the π resonance).^{26,27} Moreover, due to the hybridization with the Me d band, the adsorbate levels mix with the states at E_F of the substrate. This allows for charge-transfer screening from the substrate to the adsorbate upon ionization, and the fully screened core ionized state with the lowest energy can be envisaged as a state with a core hole and a screening electron at E_F . Provided that the

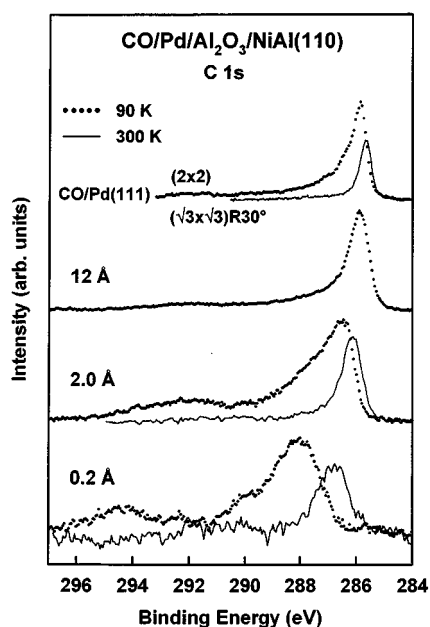


FIG. 1. C 1s XP spectra for CO adsorbed at 90 K on Pd islands of increasing size before and after heating to 300 K, compared to two ordered CO overlayers on Pd(111) (from Ref. 31). The binding energies are relative to the Fermi level of the NiAl(110) substrate.

XPS BE is measured relative to E_F , this energy pins the position of E_F in the XA spectrum and is consequently likely to be situated close to the onset of the XA threshold feature.^{27,28} This relationship is in principle expected to be observed for all metallic systems, and has been found for all studied CO chemisorption systems, including CO/Pd.²⁷ Since the photoemission process can be treated as a sudden event, the energy relationship between the x-ray photoelectron (XP) peak with the threshold feature observed in the corresponding x-ray absorption (XA) spectrum provides information about the adsorbate-substrate coupling strength and the screening response upon the sudden removal of a core electron. Consequently, this relationship can be utilized as a tool to determine whether an adsorbate system has metallic properties or not.^{29,30} In the case of a physisorbate, however, there is only negligible overlap between the adsorbate and substrate levels and no charge transfer screening is expected to occur on the time scale of the photoionization process. The relationship between the two processes is therefore not as straightforward as for chemisorbates.²⁹

Figure 1 shows C 1s XP spectra for high CO coverage on Pd islands of increasing size. For the lower Pd exposures, the spectra obtained after desorption by heating of the CO overlayer to 300 K are also shown. For comparison, C 1s spectra for two ordered phases of CO/Pd(111) are shown (from Ref. 31). Details of these spectra have been discussed elsewhere,²¹ but it is important for the coming discussion to note that the BEs increase for decreased island size.

Figure 2 depicts the corresponding C $1s \rightarrow 2\pi^*$ XA spectra for CO adsorbed on the supported islands. It has previously been observed that the width of the XA peak strongly depends on island size and CO coverage.²¹ The width of the π resonance is to a large extent a measure of the CO $2\pi^*$ -Pd $4d$ hybridization strength of the C 1s core excited state.²⁷ Thus, the hybridization width increases with increasing is-

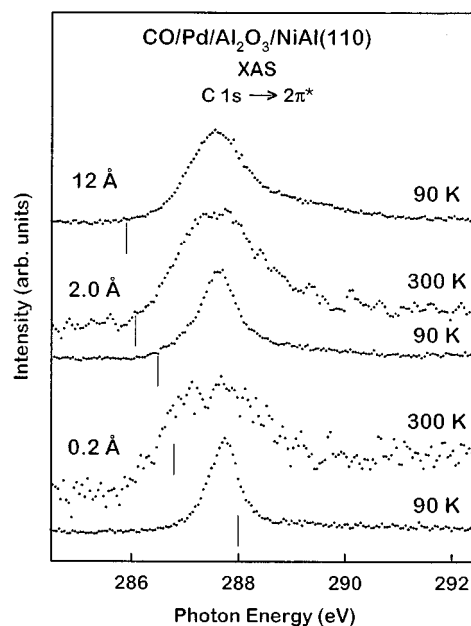


FIG. 2. C $1s \rightarrow 2\pi^*$ XA spectra for 30 L of CO adsorbed at 90 K on Pd islands of increasing average size. For 0.2- and 2.0-Å Pd, the XA spectra obtained after heating the CO overlayer to 300 K, resulting in desorption of 50–60% of the CO, are shown. The corresponding XPS BEs relative to the NiAl(110) Fermi level are marked with lines.

land size and decreasing CO coverage.

The lines in Fig. 2 represent the positions of the corresponding XPS peaks. In the case of high CO coverage, it can be seen that the XPS BE gradually moves from a position just above the XA maximum to a position near the onset of the XA peak as the island size increases. From the discussion above, it is expected that the XPS BE is situated close to the XA onset for very large amounts of Pd since this situation is expected to behave like CO adsorbed on bulk Pd.

If we then consider the small islands, we have at least one situation that is not compatible with a metallic system. TDS results show that the most weakly bonded CO molecules desorb just below 200 K.^{20,21} Based on the previous studies on CO on single-crystal surfaces, this adsorption strength is sufficient to fulfill the criteria for chemisorption.²⁷ We can therefore safely regard all the CO molecules as chemisorbed on the Pd islands, and if the XPS-XAS relationship deviates from what is expected for a metallic system, this must have an origin other than the presence of a physisorbed species.

For clusters deposited on inert surfaces, it is well known that the photoemission BE increases as the size of the cluster decreases.^{32–35} This effect is mainly ascribed to the charge left on the cluster and the shift has been found to be essentially inversely proportional to the mean radius of the cluster.^{32–35} For the Pd/Al₂O₃/NiAl(110) system, this behavior has been observed for the Pd $3d$ levels for the clean islands as well as for both the Pd $3d$ and the C 1s levels upon CO adsorption (see Fig. 1 and Ref. 21). The energy of the C $1s \rightarrow 2\pi^*$ process monitored by XAS, on the other hand, does not exhibit this kind of shift since no electron is removed from the system. The variations in the XPS-XAS relationships observed in Fig. 2 can therefore be ascribed mainly to size effects of the CO-Pd complexes.²¹ We may

also note that if there was an interaction between the CO-Pd complex and the electron reservoir of the NiAl substrate comparable to that of a chemisorbate on a metal, charge-transfer screening of the CO-Pd complex would occur on the time scale of the core ionization process and the XPS BE would in all cases appear near the XA onset. Since this is apparently not the case, it is feasible to assume that the screening is in all cases limited to what is provided by the CO-Pd complex itself with an additional contribution of image screening from the oxide film and its substrate.

Consequently, we can conclude that about 100 Pd atoms (2.0 Å) are sufficient to provide a screening upon core ionization that is (nearly) as efficient as for the bulk metal, independent of CO coverage. The only deviation is that the XPS BE for 2.0 Å is not quite connected to the XA onset, which is the case for 12 Å. That the difference between the two coverages is very small is not too surprising, since the valence photoemission (PE) spectrum for the 2.0-Å situation without CO adsorbed displays a significant intensity close to the Fermi level.²⁰ This is indicative for metallic properties of the clean Pd clusters; i.e., full screening may take place upon ionization.

For islands consisting of roughly 10 Pd atoms, it was found that the core ionization energy is slightly larger than the core excitation energy for high CO coverage, whereas for low CO coverage it is slightly lower, but still well above the XA onset. The overall nonmetallic behavior is in line with the valence PES results, which show that these islands do not exhibit metallic properties without CO.²⁰ The question is whether the electronic properties of the whole CO-Pd complex vary or if the properties of the Pd islands are constant and the effects are only due to differences in coupling strength between two (or more) different CO species. A clue to this is given by the previous XPS results, which show no intensity in the C 1s spectrum taken before heating at the position of the peak observed after heating (Fig. 1). If the same strongly coupled species was present in both cases, the BE must have shifted more than 1 eV. Such a shift cannot be explained solely by reduced CO-CO repulsion; it seems to be more likely that a change in relaxation energy occurs.^{21,27} Since we in this case assume that we have exactly the same species as before heating, minus some surrounding molecules, this evidently entails a change in the relaxation of the Pd atoms.

The other possibility is that removal of CO allows for the remaining molecules to coordinate more strongly to the Pd islands; i.e., we obtain a CO-Pd complex with a stronger CO-Pd interaction. Although we cannot distinguish between these scenarios, the conclusion is in both cases that the electronic properties of the *whole CO-Pd complex* seem to depend on the CO/Pd ratio for these limited sizes. The CO left after heating to 300 K hybridizes more strongly with the Pd atoms, and it is reasonable to believe that a system with more ‘Pd character’ can effectively rearrange charge in order to screen the core hole and reduce the core ionization energy.

It is furthermore interesting to compare the XPS and XAS values for CO adsorbed on the small islands with those of a carbonyl, which is done in Table I for high CO coverage. We note that the 0.2-Å Pd situation has an XPS-XAS relation very similar to Fe(CO)₅,^{2,12} thereby confirming the more ‘molecular’ character of this situation.

TABLE I. C 1s binding energies (BE’s) relative to the Fermi level of the NiAl(110) substrate, photon energies (PE’s) of the corresponding C 1s→2π* XA peak and the estimated spectator shifts (i.e., the shifts between the AI and AE spectra) for CO on two coverages of UHV deposited Pd (high CO coverage) and the low coverage situation of the Pd carbonyl compound. Values for condensed Fe(CO)₅ (from Refs. 2 and 12) properly adjusted for differences in the reference level are shown for comparison.

	C 1s BE (eV)	C 1s→2π* PE (eV)	Spectator shift (eV)
CO/0.2 Å Pd	288.0	287.7	2.2
CO/2.0 Å Pd	286.5	287.6	0.8
0.5 Å Pd _x (CO) _y	288.0	287.7	2.0
Fe (CO) ₅	288.3	287.8	2.8

However, there is one uncertainty concerning the validity of the XAS-XPS relations, especially for large amounts of CO adsorbed on 0.2-Å Pd: The CO molecules interact rather weakly with the Pd islands, but even though the molecules are chemisorbed, it is not certain that the strong peak observed in the XP spectrum really represents the core ionized state with the lowest energy. For systems where CO is weakly bonded, such as on Cu and Ag, shakeup satellites dominate the spectrum and the XPS peak with the lowest BE has only a very low relative intensity.^{7,8,11} Hence there is a possibility that we cannot discern the component with lowest BE; i.e., the ‘true’ XPS value is lower. In order to establish whether or not this is the case, we have employed core-hole decay techniques.

2. Decay of core excited and core ionized states

A state with a core hole is highly unstable, and it will rapidly decay by electron or photon emission. The former type of decay normally dominates, and this is the process that will be considered here. By comparing the decay of the neutral core excited state, i.e., the AI spectrum, with that of the core ionized state (the Auger electron spectrum), the screening dynamics occurring *within the core-hole lifetime* (typically 10⁻¹⁵ s) can be observed.^{12,15,16,36-40} For a free CO molecule, the AI spectrum is recorded at an excitation energy corresponding to a core to 2π* transition, i.e., the energy of the π resonance observed with XAS. The AI spectrum consists of two-hole-one-particle (2h-1p) states (spectator peaks) and single-hole (1h) states (participator peaks).^{12,40} The AE spectrum, however, only consists of 2h states. These are shifted towards lower kinetic energies (KE) relative to the 2h-1p states in the AI spectrum due to the absence of screening from the spectator electron in the 2π* orbital. Thus, the AI and AE spectra are fundamentally different.

For CO chemisorbed on a metal, the strong coupling of the 2π* orbital with the metal states quenches this difference, leading to AI and AE spectra that are nearly identical.^{14-16,37,38,41} The fact that the spectral shape is independent of excitation energy is due to the mixing between adsorbate and substrate orbitals. This leads to a decoupling of the intermediate state in terms of a local core-hole state and some additional excitation, mainly in the substrate, which has only a small influence on the decay. This can be described in terms of a decay of the intermediate state to the

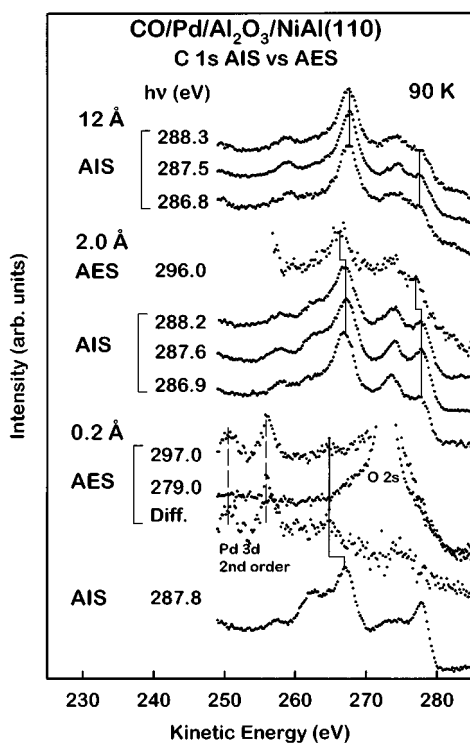


FIG. 3. C 1s decay spectra recorded at different photon energies for 30 L of CO adsorbed at 90 K on increasing amounts of Pd. In the 0.2 Å case, peaks due to direct photoemission processes excited by first- (O 2s) and second- (Pd 3d) order radiation are indicated.

lowest core excited state with an additional excitation, which is removed from the core-hole site. Alternatively, this can be explained by the fact that all the excited states within the core to valence resonance, including the lowest one, are constructed from the delocalized orbitals, which are very similar on the core-hole site. This leads to essentially the same spectator shift for all excited states and hence to deexcitation spectra that are largely independent of the detailed excitation energy.

For physisorbates, the decay spectra are basically identical to the ones in the gas phase, albeit shifted towards higher kinetic energies due to image screening, e.g., Refs. 29, 36, and 39. An important effect to be taken into account for these systems, however, is the possibility for tunneling of an electron to or from the adsorbate in order to reach the energetically most favorable core-hole state.^{36,39} This process can occur on a time scale of fs and can in such cases be observed in the decay spectra.³⁹

Figure 3 shows the C 1s decay spectra recorded at different excitation energies for 30 L CO adsorbed at 90 K on increasing amounts of Pd. The corresponding results obtained after heating to 300 K (only for 0.2 and 2.0 Å) are presented in Fig. 4. Unless otherwise indicated, features due to direct photoemission have been subtracted using a spectrum recorded below threshold. The first, general observation to be made in Figs. 3 and 4 is that all the spectra show an overall shape that is typical of coordinated CO, i.e., carbonyls and CO chemisorbed on metals, thus supporting the conclusions made in Sec. III A 1.

Focusing on the 0.2-Å situation at high CO coverage (Fig. 3), we note that the AI spectrum ($h\nu=287.8$ eV) differs from

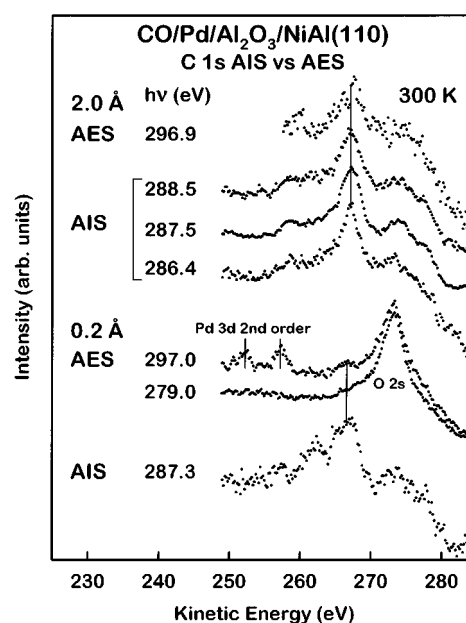


FIG. 4. C 1s decay spectra for CO adsorbed on 0.2- and 2.0-Å Pd after heating to 300 K recorded at different photon energies.

the corresponding spectrum for CO on a Pd single crystal [see Ref. 16 and the CO/Pd (111)-like 12-Å situation in Fig. 3]: The features at KE's of 263 and 278 eV, respectively, have significantly higher relative intensities for CO/0.2 Å (90 K). The peaks near the high KE edge in the AI spectra for CO adsorbed on *d* metals have been interpreted as due to a decay involving the CO $2\pi^*$ -Me *d* orbital, leading to $(4\sigma,5\sigma,1\pi)^{-1}2\pi^{-1}$ final states, whereas the features at KE's of 260–270 eV are derived predominantly from $5\sigma^{-1}1\pi^{-1}$, $1\pi^{-2}$, and $4\sigma^{-1}1\pi^{-1}$ configurations.^{15,16,42,43} Since the intensity of the peaks appearing in the decay spectrum is strongly dependent on the orbital overlap with the site of the core hole in the core excited state (the so-called one-center approximation^{44,45}), the more narrow and intense high KE features observed for carbonyls and weakly bonded CO as compared to strongly bonded CO have been explained in terms of a weakening of the CO-Me hybridization and/or an increased localization of the $2\pi^*$ -*d* hybrid orbital on the CO molecule.^{16,30}

It is furthermore most feasible that modifications of one π orbital also strongly affect the other π orbitals. Recent x-ray emission spectroscopy (XES) studies of CO/Ni(100) (Refs. 46 and 47) indicate that the whole π system (1π and $2\pi^*$) is strongly altered upon adsorption, leading to states quite different from those of the free CO molecule. We can therefore expect to see changes in the decay involving 1π along with the changes in the $2\pi^*$ decay processes, giving rise to spectral changes also at lower KE's. When comparing different adsorption systems, we find that a decreasing adsorption strength results not only in changes in the high KE region; there is also a gradual change in the spectral shape at 260–270 eV KE.^{12,16,30,43} For CO strongly chemisorbed on metal surfaces, this KE region is dominated by a single feature, whereas weakly chemisorbed CO and carbonyls exhibit a doublet instead. The ultimate case is free CO, where this part of the AI spectrum shows two strong peaks of equal intensity.^{12,40} We therefore interpret this joint effect as due to

changes in the decay channels involving π states. These types of variations in the shape of the AI spectrum are exactly what is observed in Fig. 3 for decreasing amounts of Pd, and it can therefore be concluded that the effective size of the CO-Pd complex and the strength of the CO-Pd interaction are clearly manifested in the shape of the AI spectrum.

The spectrum recorded at a photon energy of 297.0 eV represents the AE spectrum, i.e., the decay spectrum of a core-ionized species. In Fig. 3, the raw data are compared to a direct photoemission spectrum recorded at a photon energy just below the XA threshold and aligned to the O $2s$ peak in the spectrum recorded at $h\nu=297.0$ eV. The difference between these two spectra is also shown. Unfortunately, features other than the most prominent one are most difficult to discern. However, the peaks in the AE spectrum seem to be shifted about 2.2 eV towards lower KE's relative to the corresponding peaks in the AI spectrum, which we interpret as due to a spectator shift. This conclusion is supported by the spectator shifts observed for condensed carbonyls, which are of the same order of magnitude [e.g., 2.8 eV for $\text{Fe}(\text{CO})_5$, see Table I].¹² Thus, as for the carbonyl, the AE spectrum can be assumed to consist of $2h$ states whereas the AI spectrum consists of $2h$ states screened by an electron in the $2\pi^*-d$ orbital.

The finding of a situation that displays a spectator shift is important. It shows that there is no detectable charge transfer to the CO-Pd complex occurring during the core-hole lifetime. This of course implies that there is no charge-transfer screening taking place upon core ionization, which is a much faster process. Consequently, there is no 'fully screened' peak in the XP spectrum, supporting the XPS-XAS relation presented in Fig. 2. It is also evident that the influence from the substrate is limited, and there is no observable effect due to electron tunneling to the Pd island. This information is vital for the general discussion of the electronic properties of a thin oxide film grown upon a metallic substrate versus the bulk oxide, as will be further elaborated in Sec. III C.

In the previous section it was found that a lowering of the amount of CO adsorbed on the smallest islands results in a significant lowering of the core ionization energy, probably due to an enhanced ability for charge rearrangements within the CO-Pd complex. The core-hole decay spectra for low CO coverage also exhibit different characteristics as compared to high CO coverage. As observed in Fig. 4, there is no indication of a spectator shift. Possible reasons for this are that the screening of the doubly ionized Auger final states provided by charge rearrangements within the CO-Pd complex is as efficient as that of the singly ionized AIS final states or, which we find more unlikely, that the probability for electron tunneling from the substrate has strongly increased. Unfortunately, we cannot distinguish between these possibilities.

Nevertheless, we may conclude that the AIS and AES results for CO-Pd complexes consisting of approximately 10 Pd atoms are consistent with the interpretation that was made based on the XAS and XPS data: Adsorption of large amounts of CO brings about a "carbonyl-like" behavior, whereas a more "metalliclike" situation is found for a lower CO coverage.

The next situation to be discussed is the one with large amounts of CO adsorbed on 2.0-Å Pd, i.e., islands where the number of Pd atoms is of the order of 100 (Fig. 3). Starting

with the AI spectrum recorded at the XA maximum energy, we find that this spectrum more resembles the CO/bulk Pd case, although there is still a slight enhancement of the features at KE's of 263 and 278 eV. The KE shift between the AI and the AE spectra can furthermore be estimated to be around 0.8 eV, and there are small changes in relative peak intensities in the spectra recorded at photon energies within the π resonance (286.9–288.2 eV). Concerning the variations observed at excitation energies within the region of the XA peak, effects due to excitation of molecules occupying different adsorption sites might occur. However, this interpretation is not supported by the data shown at the top of Fig. 3. These represent three spectra recorded at different energies within the π resonance for 30-L CO/12-Å Pd (90 K). This is a situation very similar to CO/Pd(111) (2×2),²¹ where CO is assumed to occupy both on-top and hollow sites.^{48,49} The presence of different sites has obviously a negligible effect on the shape and the position of the AI spectrum. This is supported by AIS studies of CO/H/Ni(100), where the C $1s$ AI spectrum was found to be insensitive to the adsorption site, whereas significant effects were observed in the O $1s$ AI spectrum.¹⁶

A more feasible explanation for the relative intensity variations in the core-hole decay spectra is instead that the $2\pi^*-d$ orbital for CO adsorbed on the islands has slightly different properties than for CO adsorbed on a metal surface. If the CO/Pd ratio is of the same order of magnitude as for carbonyls, the $2\pi^*-d$ interaction results in the formation of discrete molecular orbitals rather than a continuous band. That this can lead to photon-energy-dependent variations in the decay spectra can be explained as due to an increased influence of the $2\pi^*-d$ states on the decay.

In Fig. 3 it can be seen that the main variations in the spectral shape take place at KE's of 263 and 277.5 eV, for which the intensity increases when the photon energy is increased from 286.9 to 287.6 eV (the latter value corresponds to the XA maximum). As previously inferred, such an effect can occur when the size of the system or the CO-Me interaction decreases, i.e., when the molecular character of the $2\pi^*-d$ orbital increases. That this is observed in the AI spectra when scanning through the π resonance for the same system can therefore be taken as an indication for a larger CO $2\pi^*$ character of the states close to the XA maximum as compared to those at the XA onset. In fact, the increased intensity at 278 eV can be caused by an enhanced probability for a participator decay process. This type of decay involves the excited electron and results in $1h$ final states, similar to the final states reached in photoemission.^{12,40} The difference between the photon energy and the kinetic energy of the participator peak should be equal to the BE observed by photoemission. In this case we obtain $287.6-277.5=9.1$ eV, which is close to the BE observed for the $5\sigma/1\pi$ peak (8.5 eV).¹⁹ Since the participator process leading to a $1\pi^{-1}$ state is by far the strongest in the case of free CO,^{12,40} there is reason to believe that this peak is most sensitive to an increased probability for participator decay. The possible presence of a participator process gives further support for a localized behavior, since the excited electron has to have a significant probability to populate the core-hole site in order to take part in the decay.

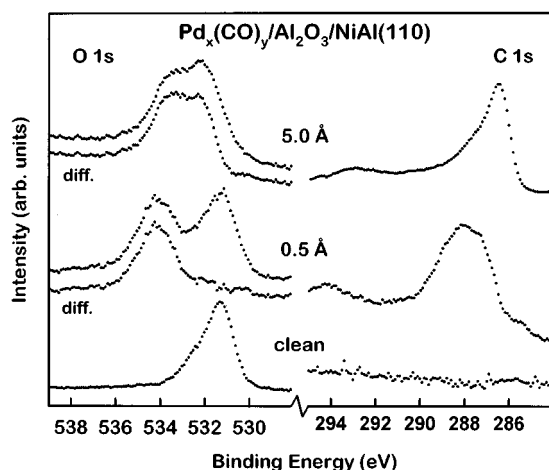


FIG. 5. C 1s and O 1s XP spectra for 0.5- and 5.0-Å $\text{Pd}_x(\text{CO})_y$. O 1s difference spectra after subtraction of oxide features are also shown. The BEs are relative to the NiAl(110) Fermi level.

Furthermore, the shape of the AE spectrum resembles the spectrum recorded at 286.9 eV more than the spectrum recorded at 287.6 eV, which is most clearly seen at the high KE side. A tentative explanation of this is that the screening charge from the metal is preferably transferred to the lowest unoccupied $2\pi^*$ -d states. Consequently, the charge distribution near the core hole for the “C 1s \rightarrow XA onset” situation and the charge-transfer-screened C 1s ionized state becomes similar, although the overall charge on the CO-Pd complex is of course different in the two cases.

It should be noted, however, that an explanation for the photon energy dependence in terms of different CO-adsorption sites cannot be excluded. The effects of different sites might be larger for the small islands as compared to the (111) surface. Nonetheless, it should be emphasized that even though this situation has approached the metallic case, the presence of an AIS-AES shift demonstrates that some molecular character is retained.

The decay spectra obtained after partial desorption of CO are presented in Fig. 4. We note that the spectra line up on a kinetic energy scale within experimental error and that the spectra appear to be identical to CO/bulk Pd. The increased tendency for metallic behavior of the CO-Pd complex for decreased CO coverage is consistent with the valence photoemission results for the clean Pd islands, showing metallic properties (cf. Sec. III A 1 and Ref. 20). Thus, the increased metallic character of the $2\pi^*$ orbital allows for a more efficient screening.

B. Growth of the $\text{Pd}_x(\text{CO})_y$ compound

It has recently been demonstrated that a palladium carbonyl-like compound [$“\text{Pd}_x(\text{CO})_y”$] can be grown upon the alumina film by vapor deposition of Pd in CO atmosphere.^{18,19} TDS and photoemission show that the compound exists for coverages ranging from fractions of a monolayer up to multilayers. Furthermore, the compound appears to have a relatively well-defined local structure and, based on the BE shifts of the Pd 3d level, it was proposed that Pd-Pd bonds form during the growth.

In this study, we have chosen to compare the properties of two different exposures, 0.5 and 5.0 Å. The low-coverage

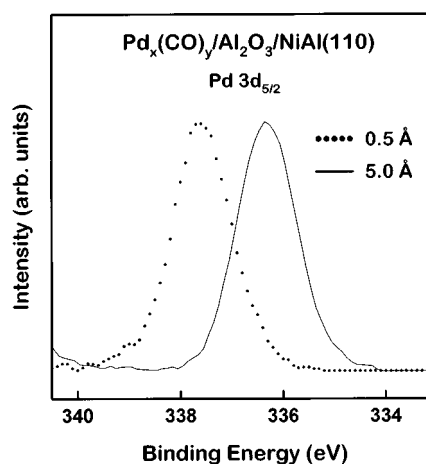


FIG. 6. Pd $3d_{5/2}$ XP spectra for 0.5 (dotted) and 5.0 Å (solid line) $\text{Pd}_x(\text{CO})_y$. The BEs are relative to the NiAl(110) Fermi level.

situation involves partial coverage of the oxide surface and a crude estimation of the island size yields an average diameter of 20 Å, consisting of roughly 40 Pd atoms.^{19,25} For the higher dose, the whole surface is covered.^{18,19}

1. The Pd-CO bonding geometry

The CO-related core-level photoemission spectra for the two situations compared to the clean oxide film are presented in Fig. 5, including O 1s difference spectra after removal of the oxide features. The corresponding Pd $3d_{5/2}$ peaks are shown in Fig. 6. Starting with the O 1s data, the 0.5-Å situation shows one broad peak, whereas two features are observed at 5.0 Å. The C 1s spectra exhibit the same behavior although not as pronounced; at 5.0 Å the high BE component appears only as a shoulder on the low BE component. Using a simple curve fitting procedure, the BE's, relative areas, and widths of the peaks have been estimated and the results are presented in Table II.

Since the Pd 3d spectra contain only one symmetric peak, the appearance of two components in the C 1s and O 1s spectra is probably not due to different carbonyl species or a layer-dependent electrostatic shift. Further support for this conclusion can be found in an extensive discussion given in Ref. 19. We instead attribute the two components in the C 1s and O 1s spectra for the 5.0-Å case to CO adsorbed in two

TABLE II. C 1s and O 1s binding energies (BE's) relative to the Fermi level of the NiAl(110) substrate for two coverages of the Pd carbonyl compound. The fitted widths, relative areas, and proposed adsorption geometries are also given. FWHM denotes full width at half maximum.

Exposure	BE (eV)	FWHM (eV)	Area	Site
0.5 Å	534.1	1.8	0.9	Terminal
O 1s	532.9	(1.6)	(0.1)	Bridge
C 1s	288.0	2.7	1	Terminal
5.0 Å	533.4	1.8	0.6	Terminal
O 1s	532.0	1.3	0.4	Bridge
C 1s	287.1	2.2	0.6	Terminal
	286.3	1.0	0.4	Bridge

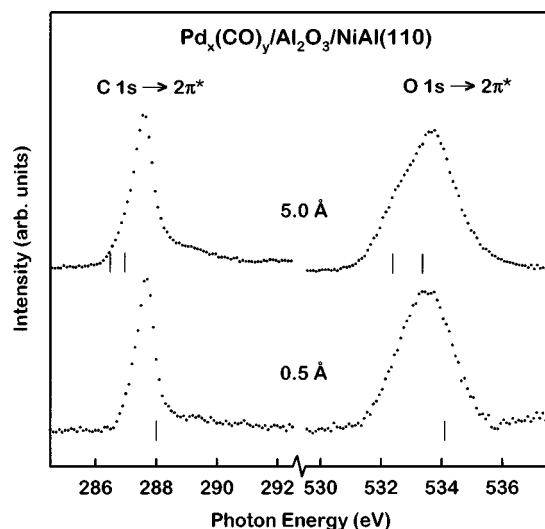


FIG. 7. C $1s \rightarrow 2\pi^*$ and O $1s \rightarrow 2\pi^*$ XA spectra for 0.5- and 5.0-Å $\text{Pd}_x(\text{CO})_y$. The O $1s$ spectra are those obtained after subtraction of oxide features. The corresponding XPS BEs relative to the NiAl(110) Fermi level are marked with lines.

different bonding geometries, since the magnitude of the splitting observed in the O $1s$ spectrum is comparable to the O $1s$ shifts previously observed for CO adsorbed in different sites, both for CO adsorbed on single crystal surfaces and for carbonyls.^{2,50–55}

In order to assign the O $1s$ peaks to specific sites, we can compare our BE's to those found for well-defined rhodium carbonyls deposited on alumina and graphite.⁵¹ The C $1s$ and O $1s$ BE's for the 0.5-Å situation, which would most resemble the situation of a deposited small carbonyl molecule, are in perfect agreement with the values for terminally bonded CO. Furthermore, the shifts between the two components in the 5.0-Å spectra (O $1s$: 1.4 eV, C $1s$: 0.8 eV) are comparable to the shifts towards lower BE's when going from terminally to bridge-bonded CO for Rh carbonyls (O $1s$: 1.5–2.0 eV, C $1s$: 0.7–1.1 eV).⁵¹

XA spectra are presented in Fig. 7, showing the C $1s$ and O $1s$ π resonances for the two different Pd exposures. The C $1s$ XA peak is in both cases found to be narrow, with no clear evidence for a doublet structure. In the O $1s$ spectra, however, one peak is found at an exposure of 0.5 Å whereas the 5.0-Å spectrum exhibits a shoulder at the low photon energy side, consistent with the population of two different CO sites in the latter case.⁵⁶ That this effect is difficult to observe in the C $1s$ spectra is due to the following reasons (a) The separation is expected to be smaller. (b) The XA peak associated with a higher coordination is expected to be broader due to a stronger CO $2\pi^* - \text{Me } d$ hybridization in the core excited state, as previously demonstrated for CO adsorbed on metals.^{27,56} (c) Finally, the XA peak for the more highly coordinated CO species could also have a lower intensity due to, for instance, a lower number of unoccupied $2\pi^* - \text{Me } d$ states.⁵⁶

The XPS and XAS results thus indicate that the $\text{Pd}_x(\text{CO})_y$ compound consists mainly of CO adsorbed in terminal sites at low coverages, whereas at high coverages bridge sites are also populated. However, as indicated by previous results, the thermal stability of the compound does not vary with

coverage.^{18,19} This is indicative of no significant changes in the bonding strength within the Pd-CO complex, at least for the terminally bonded species (since it is the only one present at lower coverages).

2. The change from a molecular system towards a metallic system

After elucidating the geometrical structure of the CO-Pd bonding, we will now turn to the screening properties with respect to the size of the $\text{Pd}_x(\text{CO})_y$ islands. The XPS BE's are shown as lines in Fig. 7. For the 0.5-Å case, we find for both C $1s$ and O $1s$ that the XPS BE appears slightly above the XA maximum and not in connection to the onset. Thus, the energy of the core-ionized state is larger than the energy required to create a neutral, core-excited state; i.e., the XPS final states are not fully screened. We also note that the XPS and XAS energies are very similar to the CO/0.2-Å Pd case at high CO coverage (Table I).

For the higher coverage (5.0 Å), however, the C $1s$ BE's appear near the XA onset and the O $1s$ BE's are clearly below the corresponding XA maxima, as for CO adsorbed on a metal. That the O $1s$ BE appears closer to the XA maximum is an effect of the interplay between the hybridization broadening and the intramolecular vibrational broadening (which is substantial for O $1s$ excited states) of the XAS line profile.²⁷ For CO chemisorbed on a metal, the O $1s$ BE will never appear above the XA maximum. Consequently, the positions of the XPS peaks relative to the corresponding XA features observed for 5.0 Å may indicate fully screened core-ionized states.

C $1s$ decay spectra for the two coverages of the $\text{Pd}_x(\text{CO})_y$ compound recorded at several photon energies are presented in Fig. 8. Beginning with the 0.5-Å situation, the ionization limit (the vacuum level) has been estimated to be at 293 eV. It is readily observed that the spectrum recorded at a photon energy exceeding this value (i.e., the AE spectrum) is shifted about 2.0 eV towards lower KE, which we attribute to a spectator shift. The C $1s$ decay spectra are indeed very similar to those previously reported for condensed carbonyls as well as the CO/0.2-Å Pd situation discussed above. The spectator shift also appears to be of the same magnitude.¹² In Table I we compare the C $1s$ XPS, XAS, AIS, and AES results for 0.5 Å of the $\text{Pd}_x(\text{CO})_y$ compound with those of the small UHV-deposited islands and $\text{Fe}(\text{CO})_5$.¹² The results convincingly demonstrate that the islands obtained after a deposit of 0.5 Å $\text{Pd}_x(\text{CO})_y$ behave like deposited carbonyl molecules.

Other interesting observations that can be made using Fig. 8 are that the peaks at KE's of 263 and 278 eV show an increased relative intensity as the photon energy reaches the value of the XA maximum and that the shape of the spectrum recorded below the XA maximum resembles that of the AE spectrum, which was also observed for high CO coverage on 2.0-Å Pd. Furthermore, a similar effect can also be found when comparing the previously reported AI and Auger spectra for carbonyls, i.e., the relative intensity of the feature with highest KE is lower in the Auger spectrum than in the AI spectrum,¹² but variations in the spectral shape appearing at excitation energies within the π resonance have so far not been reported.

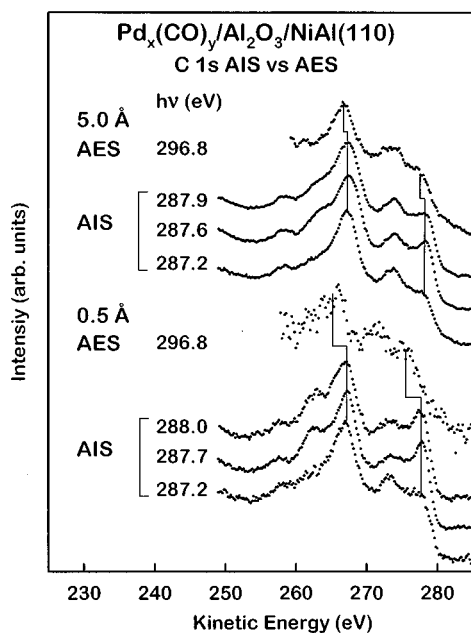


FIG. 8. C 1s decay spectra for 0.5-Å and 5.0-Å $\text{Pd}_x(\text{CO})_y$ recorded at different photon energies.

In line with the discussion made for the 2.0-Å situation at high CO coverage (Sec. III A 2), we attribute these variations to the possibility for creation of core-hole states with different charge distributions. However, we feel more confident about the interpretation in this case, since, at this coverage, CO adsorbed in terminal sites totally dominates, thus excluding the possibility for excitation of different CO species. It can therefore be concluded that the photon-energy-dependent effects seen in Fig. 8 is a general effect caused by the $2\pi^*-d$ mixing and are expected to occur for all transition metal carbonyls.

Moreover, the increased intensity at a KE of 278 eV is again compatible with the appearance of participator decay, since the $1h$ BE obtained by subtracting the KE from the used PE (287.7 eV) yields 9.7 eV, which is in good agreement with the BE of 9.3 eV observed for the $5\sigma/1\pi$ peak in the valence PE spectrum.^{18,19} Since the 1π participator peak for free CO is the strongest, it is possible that the increased intensity around 278 eV is the result of 1π participator decay.

Regarding the high-coverage case (5.0 Å), the XP and XA spectra indicated that full screening of the core-ionized states occurs within the time scale of the photoemission process. If this is true, we would expect no or only very small differences in the core-hole decay spectra as a function of photon energy, as for CO/metals. This is almost the case, as demonstrated in Fig. 8; the KE shift between the AI and the AE spectra is below 0.4 eV. We can therefore conclude that the screening properties for large amounts of the $\text{Pd}_x(\text{CO})_y$ compound have approached those of an extended, metallic system, but some molecular character is still remaining.

The observations for the two different coverages support the idea of Pd-Pd bond formation during the growth: At low coverage, the $2\pi^*-4d$ hybrid orbital is confined on the island with no possibility to receive an external screening electron from the substrate in order to screen the CO molecule upon

core ionization. At high coverage, the $\text{Pd}_x(\text{CO})_y$ compound covers the whole surface, connected by Pd-Pd bonds, and can effectively transfer an electron to the core ionized site. Consequently, the $2\pi^*-4d$ orbital is expected to have a more delocalized character for high coverages, which would to a large extent decrease the possibility for participator decay.¹⁶ Upon close inspection of Fig. 8, we find that the intensity variations at KE's 263 and 278 eV still remain but appear to weaken. However, since the CO molecules in this case occupy two different sites, this could also affect the shape and relative intensities of the spectrum, although these effects are expected to be rather small in the C 1s decay spectra as realized for CO on metals.¹⁶

C. Influence from the substrate

A key issue when comparing the properties of the thin alumina film versus bulk alumina is the influence of the metallic substrate underneath the oxide film. Can electrons tunnel from the metal to the deposited islands through the oxide layers and give it properties different from islands on the bulk oxide? We would like to briefly broach this subject.

The question of an electron tunneling effect can be raised in connection with two situations: the high CO coverage phase on 0.2-Å Pd and 0.5-Å $\text{Pd}_x(\text{CO})_y$. Since tunneling occurs in order to create the energetically most favorable core-hole state, this would in both cases lead to the appearance of AI features in the AE spectrum with an intensity proportional to the charge transfer rate.³⁹ The AE spectrum for CO/0.2-Å Pd suffers from intensity problems (Fig. 3), but it can be concluded that the decay from an ionic state dominates. The AE spectrum for 0.5-Å $\text{Pd}_x(\text{CO})_y$ (Fig. 8) is of higher quality and although it is clear that the ionic decay dominates also in this case, the AE spectrum is found to be slightly broader than the AI spectrum. Assuming that the broadening is due to a contribution from a decay from a charge transfer screened state, a simple modeling using two shifted AI spectra ($h\nu=287.2$ eV) yields a rough estimation of about 25% as an upper limit for the charge-transfer screened part. However, for a thick condensed carbonyl film, i.e., a case where the substrate-induced effects are negligible, the AE spectrum is also found to be broader than the corresponding AI spectrum.^{1,12} The AE spectrum is recorded with an excitation energy high above threshold, and it is therefore possible that high-energy core-hole states ("shakeup states") may contribute, leading to a broadening of the spectrum towards the high KE side.¹ Moreover, AIS and AES data for CO adsorbed directly on $\text{Al}_2\text{O}_3/\text{NiAl}(110)$ show no conclusive evidence for a tunneling effect.⁴³ On the other hand, in the case of $\text{SF}_6/2$ ML $\text{NaCl}/\text{Ge}(100)$ a high KE feature was observed in the AE spectrum and interpreted as stemming from a charge-transfer process from the $\text{Ge}(100)$ substrate.⁵⁷ Evidently, two layers of NaCl, which is a thickness comparable to the alumina film,²³ between the adsorbate and the metal was not enough to completely close the charge-transfer channel. This system, however, may have substantially different chemical properties. We therefore find it most likely that for CO/ $\text{Pd}/\text{Al}_2\text{O}_3/\text{NiAl}(110)$, the influence from the NiAl(110) substrate upon a strong perturbation in the electronic structure of the islands is very small on a time scale of fs, implying that electron tunneling effects from the metallic

substrate can be disregarded when probing the system with fast processes (such as photoemission).

IV. CONCLUSIONS

We have investigated two alternative methods to experimentally monitor the development of a CO adsorption system that gradually changes from localized to delocalized: Firstly by studying CO adsorbed on Pd islands of increasing size deposited under UHV conditions and secondly by studying the growth of a Pd carbonyl-like species, formed by Pd deposition in CO atmosphere. The substrate was in both cases a thin alumina film grown upon NiAl(110). Of major interest was the change in screening properties as a function of the number of metal atoms. X-ray photoelectron spectroscopy (XPS) and x-ray absorption spectroscopy (XAS) were used to determine the screening response upon a sudden removal of a core electron whereas AES and AIS were used to investigate the screening dynamics on the time scale of the core-hole lifetime (10^{-15} s).

For the UHV-deposited islands, we find that the electronic properties of the CO-Pd complexes are strongly dependent on both island size and CO coverage: Adsorption of large amounts of CO yield a screening ability that is strongly reduced, and small effects characteristic of molecular systems can be detected even for islands with ~ 100 Pd atoms. A low CO coverage, however, allows for a screening nearly as efficient as for metallic systems even for the smallest islands (of the order of 10 Pd atoms).

The carbonyl-like compound evidently entails formation of Pd-Pd bonds. It has a relatively well-defined local structure and new, complementary data concerning the CO adsorption geometries were presented. The results furthermore demonstrate that this compound undergoes a transition from a molecular to an extended system for increasing coverages, and may therefore also serve as an important link between a carbonyl and CO adsorbed on a metallic surface.

Finally, the results show that the influence from the NiAl substrate upon strong changes in the charge distribution can be disregarded if the perturbation takes place within fs. This is important when discussing the electronic properties of the thin alumina film versus bulk alumina and the applicability of the former to the construction of a model catalyst.

ACKNOWLEDGMENTS

We thank the staff at MAX Lab for invaluable experimental assistance. This work was funded by Deutsche Forschungsgemeinschaft, Ministerium für Wissenschaft und Forschung des Nordrhein-Westfalen, Fonds der Chemischen Industrie, the Swedish Natural Science Research Council (NFR), and the National Board for Industrial and Technical Development (NUTEK) through the Consortium on Clusters and Ultrafine Particles. A.S. wishes to acknowledge NFR for financial support and J.L. thanks the Studienstiftung des Deutschen Volkes for financial support.

*Present address: Department of Synchrotron Radiation Research, Lund University, Box 118, S-221 00 Lund, Sweden.

[†]Present address: Fritz-Haber-Institut der Max-Planck-Gesellschaft, Faradayweg 4-6, D-141 95 Berlin, Germany.

¹*Applications of Synchrotron Radiation*, edited by W. Eberhardt, Springer Series in Surface Sciences Vol. 35 (Springer, Berlin, 1994), and references therein.

²E. W. Plummer, W. R. Salaneck, and J. S. Miller, *Phys. Rev. B* **18**, 1673 (1978).

³J. Bustad, C. Enkvist, S. Lunell, H. Tillborg, A. Nilsson, S. Osborne, A. Sandell, N. Mårtensson, and S. Svensson, *Chem. Phys.* **179**, 303 (1994).

⁴H.-J. Freund and E. W. Plummer, *Phys. Rev. B* **23**, 4859 (1981).

⁵A. Nilsson and N. Mårtensson, *Phys. Rev. B* **40**, 10 249 (1989).

⁶J. C. Fuggle, T. E. Madey, M. Steinkilberg, and D. Menzel, *Chem. Phys. Lett.* **33**, 233 (1975).

⁷P. R. Norton, R. L. Tapping, and J. W. Goodale, *Surf. Sci.* **72**, 33 (1978).

⁸C. R. Brundle, P. S. Bagus, D. Menzel, and K. Hermann, *Phys. Rev. B* **24**, 7041 (1981).

⁹E. Umbach, *Surf. Sci.* **117**, 482 (1982).

¹⁰A. Nilsson, N. Mårtensson, S. Svensson, L. Karlsson, D. Nordfors, U. Gelius, and H. Ågren, *J. Chem. Phys.* **96**, 8770 (1992).

¹¹H. Tillborg, A. Nilsson, and N. Mårtensson, *J. Electron Spectrosc. Relat. Phenom.* **62**, 73 (1993), and references therein.

¹²W. Eberhardt, C. T. Chen, W. K. Ford, E. W. Plummer, and H. R. Moser, in *DIET II*, edited by W. Brenig and D. Menzel, Springer Series in Surface Sciences Vol. 4 (Springer, Berlin, 1985), p. 50; W. Eberhardt, E. W. Plummer, C. T. Chen, and W. K. Ford, *Aust. J. Phys.* **39**, 853 (1986).

¹³D. R. Jennison, G. D. Stucky, R. R. Rye, and J. A. Kelber, *Phys. Rev. Lett.* **46**, 911 (1981).

¹⁴H.-J. Freund and M. Neumann, *Appl. Phys. A* **47**, 3 (1988).

¹⁵W. Wurth, C. Schneider, R. Treichler, D. Menzel, and E. Umbach, *Phys. Rev. B* **37**, 8725 (1988).

¹⁶A. Sandell, O. Björneholm, A. Nilsson, B. Hernnäs, J. N. Andersen, and N. Mårtensson, *Phys. Rev. B* **49**, 10 136 (1994).

¹⁷M. Bäumer, J. Libuda, A. Sandell, H.-J. Freund, G. Graw, Th. Bertrams, and H. Neddermeyer, *Ber. Bunsenges. Phys. Chem.* **99**, 1381 (1995).

¹⁸J. Libuda, A. Sandell, M. Bäumer, and H.-J. Freund, *Chem. Phys. Lett.* **240**, 429 (1995).

¹⁹A. Sandell, J. Libuda, M. Bäumer, and H.-J. Freund, *Surf. Sci.* **346**, 108 (1996).

²⁰A. Sandell, J. Libuda, P. A. Brühwiler, S. Andersson, A. J. Maxwell, M. Bäumer, N. Mårtensson, and H.-J. Freund, *J. Electron Spectrosc. Relat. Phenom.* **76**, 301 (1995).

²¹A. Sandell, J. Libuda, P. A. Brühwiler, S. Andersson, A. J. Maxwell, M. Bäumer, N. Mårtensson, and H.-J. Freund, *J. Vac. Sci. Technol. A* **14**, 1546 (1996); M. Bäumer, J. Libuda, and H.-J. Freund, in *NATO Advanced Studies Institute Series C: Mathematical and Physical Sciences* (Kluwer, Dordrecht, in press).

²²J. N. Andersen, O. Björneholm, A. Sandell, R. Nyholm, J. Forsell, L. Thånell, A. Nilsson, and N. Mårtensson, *Synch. Rad. News.* **4**, 15 (1991).

²³R. M. Jaeger, H. Kuhlenbeck, H.-J. Freund, M. Wuttig, W. Hoffmann, R. Franchy, and H. Ibach, *Surf. Sci.* **259**, 253 (1991).

²⁴J. Libuda, F. Winkelmann, M. Bäumer, H.-J. Freund, Th. Bertrams, H. Neddermeyer, and K. Müller, *Surf. Sci.* **318**, 61 (1994).

- ²⁵The simple estimation of the number of Pd atoms per island was obtained in the following way: Assuming fcc growth on the quartz microbalance plate, the total number of deposited atoms can be calculated. SPA-LEED results give an estimate on the average island size and the relative coverage (Refs. 17 and 19). If the basal plane of the island is assumed to be circular, the number of islands can be obtained and, consequently, the number of atoms/island.
- ²⁶Y. Jugnet, F. J. Himpsel, P. Avouris, and E. E. Koch, *Phys. Rev. Lett.* **53**, 198 (1984).
- ²⁷O. Björneholm, A. Nilsson, E. Zdansky, A. Sandell, B. Hernnäs, H. Tillborg, J. N. Andersen, and N. Mårtensson, *Phys. Rev. B* **46**, 10 353 (1992).
- ²⁸A. Nilsson, O. Björneholm, E. O. F. Zdansky, H. Tillborg, N. Mårtensson, J. N. Andersen, and R. Nyholm, *Chem. Phys. Lett.* **197**, 12 (1992).
- ²⁹A. Nilsson, O. Björneholm, B. Hernnäs, A. Sandell, and N. Mårtensson, *Surf. Sci. Lett.* **293**, L835 (1993).
- ³⁰A. Sandell, P. Bennich, A. Nilsson, O. Björneholm, B. Hernnäs, and N. Mårtensson, *Surf. Sci.* **310**, 16 (1994).
- ³¹J. N. Andersen *et al.* (unpublished).
- ³²M. G. Mason, *Phys. Rev. B* **27**, 748 (1983).
- ³³G. K. Wertheim, *Z. Phys. B* **66**, 53 (1987).
- ³⁴G. K. Wertheim, *Z. Phys. D* **12**, 319 (1989).
- ³⁵G. K. Wertheim, S. B. DiCenzo, and D. N. E. Buchanan, *Phys. Rev. B* **33**, 5384 (1986).
- ³⁶W. Wurth, P. Feulner, and D. Menzel, *Phys. Scr.* **T41**, 213 (1992).
- ³⁷C. T. Chen, R. A. DiDio, W. K. Ford, E. W. Plummer, and W. Eberhardt, *Phys. Rev. B* **32**, 8434 (1985).
- ³⁸W. Wurth, C. Schneider, R. Treichler, D. Menzel, and E. Umbach, *Phys. Rev. B* **35**, 7741 (1987).
- ³⁹O. Björneholm, A. Nilsson, A. Sandell, B. Hernnäs, and N. Mårtensson, *Phys. Rev. Lett.* **68**, 1892 (1992).
- ⁴⁰H.-J. Freund and C.-M. Liegener, *Chem. Phys. Lett.* **134**, 70 (1987).
- ⁴¹G. Illing, T. Porwol, I. Hemmerich, G. Dömötör, H. Kuhlenbeck, H.-J. Freund, C.-M. Liegener, and W. von Niessen, *J. Electron Spectrosc. Relat. Phenom.* **51**, 149 (1990).
- ⁴²T. Porwol, G. Dömötör, I. Hemmerich, J. Klinkmann, H.-J. Freund, and C.-M. Liegener, *Phys. Rev. B* **49**, 10 557 (1994).
- ⁴³J. Klinkmann, D. Cappus, K. Homann, T. Risse, A. Sandell, T. Porwol, and H.-J. Freund, *J. Electron Spectrosc. Relat. Phenom.* **77**, 155 (1996).
- ⁴⁴H. Ågren and J. Nordgren, *Theoret. Chim. Acta (Berlin)* **58**, 111 (1981).
- ⁴⁵F. P. Larkins, *J. Electron Spectrosc. Relat. Phenom.* **51**, 115 (1990).
- ⁴⁶A. Nilsson, P. Bennich, T. Wiell, N. Wassdahl, N. Mårtensson, J. Nordgren, O. Björneholm, and J. Stöhr, *Phys. Rev. B* **51**, 10 244 (1995).
- ⁴⁷P. Bennich, A. Nilsson, T. Wiell, J. Bustad, N. Wassdahl, N. Mårtensson, O. Björneholm, J. Nordgren, J. Stöhr, and S. Lunell (unpublished).
- ⁴⁸H. Conrad, G. Ertl, and J. Küppers, *Surf. Sci.* **76**, 323 (1978).
- ⁴⁹F. M. Hoffmann, *Surf. Sci. Rep.* **3**, 107 (1983).
- ⁵⁰S. C. Avancino and W. L. Jolly, *J. Am. Chem. Soc.* **98**, 6505 (1976).
- ⁵¹G. Apai and B. G. Frederick, *Langmuir* **3**, 395 (1987).
- ⁵²P. R. Norton, J. W. Goodale, and E. B. Selkirk, *Surf. Sci.* **83**, 189 (1979).
- ⁵³H. Tillborg, A. Nilsson, and N. Mårtensson, *Surf. Sci.* **273**, 47 (1992).
- ⁵⁴L. A. DeLouise, E. J. White, and N. Winograd, *Surf. Sci.* **147**, 252 (1984).
- ⁵⁵O. Björneholm, A. Nilsson, H. Tillborg, P. Bennich, A. Sandell, B. Hernnäs, C. Puglia, and N. Mårtensson, *Surf. Sci.* **315**, L983 (1994).
- ⁵⁶H. Tillborg, A. Nilsson, N. Mårtensson, and J. N. Andersen, *Phys. Rev. B* **47**, 1699 (1993).
- ⁵⁷A. Klekamp and E. Umbach, *Surf. Sci.* **284**, 291 (1993).